Neural Network Adaptive Control for Pneumatic Muscle Joint Systems with Unknown Nonsymmetric Actuator Dead-Zone

Xintong Tian, Zhao Zhang, Hongyan Zhou, and Xue-Bo Chen

***Abstract*—In this paper, the adaptive control problem of pneumatic muscle (PM) joint systems with external disturbance, reconstruction error, and actuator dead-zone is researched. Compared with the existing results, the tracking performance of the PM joint system has been enhanced, and the system now guarantees the boundedness of the actuator output. First, an adaptive neural network is used to estimate the unknown dynamical behavior and the external disturbance of the system online, enabling real-time estimation of systematic errors. A static neural network is constructed to compensate for the unknown asymmetric dead-zone nonlinearity of the actuator. Second, an online robust update term is introduced to counteract reconstruction errors of the neural network and the external disturbance. Third, the Lyapunov theory is used to derive a smooth control law, ensuring the stability of the system and rigorously proving the uniform ultimate boundedness of the weight parameters of each neural network. Finally, the feasibility and effectiveness of the proposed scheme are demonstrated through simulations.**

***Index Terms*—adaptive control, dead-zone, neural network, pneumatic muscle joint system, nonlinear control.**

I. Introduction

PNEUMATIC muscles (PMs) represent an innovative addition to the array of pneumatic components utilized in sophisticated and adaptable control systems [1]. These muscles offer distinct advantages such as operational safety, economic efficiency, and hygiene. Their constructs mimic the functionality of human skeletal muscles [2]. As pneumatic technology evolves, PMs have found widespread application in lower limb exoskeleton frameworks and robotic gait rehabilitation systems [3]. Furthermore, they hold considerable promise for use in realms such as rehabilitative medicine, virtual reality, and biomimetic robotics [4]. It is widely acknowledged that real-world systems are rife with uncertainties, including unpredictable parameters, extrinsic disturbances, and modeling inaccuracies, all of which can compromise system efficacy. Achieving precise control in the face of these challenges is a formidable task that has captivated the attention of the research community.

To mitigate potential detrimental impacts, several research findings have surfaced [5–8]. In [9–11], a methodology for ensuring tracking performance subject to user-specified output constraints has been advanced. However, should this approach be adopted, the system parameters fail to autonomously adapt in the event of abrupt parameter fluctuations.

Consequently, certain tracking methodologies have employed adaptive neural networks (NNs) or fuzzy logic control to address the system's inherent uncertainty[12–15]. In [12], NNs were utilized to approximate nonlinear functions and surmount the system's uncertainty. In [13], a Gaussian radial basis function (GRBF) neural network was amalgamated with a piecewise constant adaptive law to approximate the system's uncertainty. In [14], an adaptive neural velocity reference trajectory tracking control method for high-powered three-phase induction motors was introduced, based on an 84-pulse voltage source converter. In [15], the influence of unknown function is solved by using radial basis function neural network (RBFNN).

And significant interference can attenuate the efficacy of the system's control. To surmount this predicament, a terminal sliding mode control strategy has been promulgated in [16]. In [17], the amalgamation of sliding mode variable structure control, backward control, and adaptive control has culminated in the presentation of a novel methodology. In [18], the sensitivity of the controller to disturbances is be reduced by using sigmoid basis functions for disturbance compensation.

To address the aforementioned issues, in [4], auxiliary signals and functions have been introduced as an approximation to the $\mathrm{sign}(\cdot)$ function, aimed at addressing the unknown saturation and uncertainties arising from modeling errors. Nevertheless, it is indubitable that the controller falls short of enabling real-time trajectory tracking and eliminating errors online.

It is universally understood that the precipitous variations in system parameters typically originate from the failures of unknown actuators during the operational phase of the system [19–23]. Hence, in addition to the aforementioned uncertainties, the common nonlinear characteristics of actuators represent a critical issue. Within the realm of adaptive control for the PM joint system, the impact of the nonlinear characteristics of the actuator on the system's control performance is undeniably significant.

Common nonlinear characteristics of actuators encompass saturation, dead-zone, and hysteresis, as delineated in [24].

Manuscript received March 3, 2024; revised September 12, 2024. The research work was supported by the Fundamental Research Funds for the Liaoning Universities.

Xintong Tian is a postgraduate student of School of Computer Science and Software Engineering, University of Science and Technology Liaoning, Anshan, 114051, China. (e-mail: tianxintong025@163.com).

Zhao Zhang is an associate professor of School of Computer Science and Software Engineering, University of Science and Technology Liaoning, Anshan, 114051, China. (corresponding author, e-mail: zhangzhao333@hotmail.com).

Hongyan Zhou is a doctoral student of School of Electronic and Information Engineering, University of Science and Technology Liaoning, Anshan, 114051, China. (e-mail: zhou321yan@163.com).

Xue-Bo Chen is a professor of School of Electronic and Information Engineering, University of Science and Technology Liaoning, Anshan, 114051, China. (e-mail: xuebochen@126.com).

Notably, the dead-zone exerts a substantial influence on control performance. To mitigate this impact, various controller design methodologies have been advanced in [25, 26]. For instance, in [25], the actual control input of the system under consideration must be bounded, with the dead-zone being decomposed, mathematically transformed, and deflated. In [27], an extended state observer (ESO) is employed to estimate all external disturbances and other unknowns, albeit at the expense of reducing the system's conservatism.

In this paper, the dead-zone models presented are more generalized. It is unnecessary to ascertain whether the actual control input is bounded; instead, one need only be cognizant of the dead-zone's range. Furthermore, the majority of research has adopted the strategy of constructing a dead-zone inverse, as referenced in [28, 29], which, however, escalates the complexity of the control strategy. It is acknowledged that recurrent neural networks (RNNs) have demonstrated superior efficacy in addressing dynamic systems. Nonetheless, RNNs necessitate the resolution of fixed points at every instant, thereby augmenting the computational load.

In this paper, the dead-zone is addressed through the application of a static neural network (NN) in conjunction with the implicit function theorem. Consequently, the computational burden associated with the control is alleviated herein. In pursuit of enhancing the control performance of the PM joint system, the principal contributions are enumerated as follows:

1). An NN is used to estimate system states and external disturbances online. Different from the literature [4], it can make the system track the trajectory in real time and ensure that the error is infinitely close to 0.

2). An online update robust term is used to reduce the damage of reconstruction errors and system disturbances to the control performance of the PM joint.

3). A static NN is introduced to solve the dead-zone problem of the actuator.

4). The adaptive control method designed in this paper is applicable not only to the controller with dead-zone, but also to the controller without dead-zone. As a result, the control method has a wider range of applications.

The structure of this paper is as follows. In Section II, the system description and preliminaries are given. In Section III, the controller design method is proposed. In Section IV, the control method given in this paper is verified by simulation experiments. Finally, Section V is a conclusion.

Notation: Let R denotes the real number, R^l and $R^{l\times n}$ denote the l real vector and the $l\times n$ real matrix, respectively. $|\cdot|$ denotes the absolute value. $\|\cdot\|$ for the vector denotes the Euclidean norm of the vector, for the matrix denotes its F norm, which is defined as $\|X\| = \sqrt{\mathrm{tr}\{X^TX\}}$, where $\mathrm{tr}\{\cdot\}$ denotes the trace of the matrix.

II. System description and preliminaries

A. System description

The PM joint as shown in Fig. 1. From [4], the force and the internal pressure of the PM joint can be written as

$$\begin{cases} F_1(t) = P_{b1}(t)(k_{f1}\varepsilon_1^2(t) + k_{f2}\varepsilon_1(t) + k_{f3}) + k_{f4}, \\ F_2(t) = P_{b2}(t)(k_{f1}\varepsilon_2^2(t) + k_{f2}\varepsilon_2(t) + k_{f3}) + k_{f4}, \\ P_{b1}(t) = P_{b0} + \Delta P = k_0u_0 + k_0k_vV', \\ P_{b2}(t) = P_{b0} - \Delta P = k_0u_0 - k_0k_vV', \end{cases} \tag{1}$$

where F_1, F_2 are two pulling forces on the PM joint; P_{b1}, P_{b2} are two internal pressures of the PM joint; the initial internal pressure P_{b0} is defined; k_{f1}, k_{f2}, k_{f3} and k_{f4} are the PM joint related parameters; k_0 is a proportionality factor; k_v is the voltage distribution coefficient; the reloaded voltage u_0 is defined; ε_1 and ε_2 are ratios of contraction lengths to the initial length of the PM joint, they can be written as

$$\begin{cases} \varepsilon_1(t) = \varepsilon_0 + Rl_0^{-1}\theta(t), \\ \varepsilon_2(t) = \varepsilon_0 - Rl_0^{-1}\theta(t), \end{cases} \tag{2}$$

where R is a radius of the upper platform for the mechanism of PM; the initial shrinking rate of PM ε_0 is defined; the initial length of PM l_0 is defined. u is the input of the actuator with unknown asymmetric dead-zone; V' is the output of actuator with unknown asymmetric dead-zone, and it is defined as follows:

$$V' = D(u) = \begin{cases} m_1(u), & \text{if } u \le b_1, \\ 0, & \text{if } b_1 \le u \le b_2, \\ m_2(u), & \text{if } u \ge b_2, \end{cases}$$

where $b_1 \le 0$ and $b_2 \ge 0$ are the lower and upper bounds of the dead-zone, $m_1(u)$ and $m_2(u)$ are two unknown continuous functions outside the dead-zone.

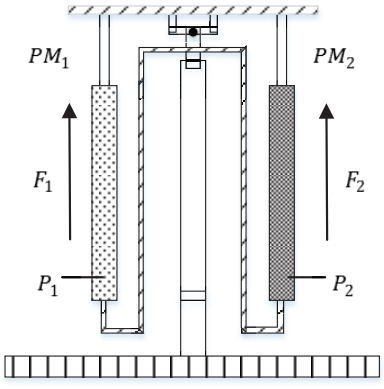

Fig. 1: The mechanism of the PM joint.

According to the law of rotation, we have

$$T(t) = I_c\ddot{\theta}(t) + K_d\dot{\theta}(t) = F_1(t)r_1 - F_2(t)r_2 + \eta(t), \tag{3}$$

where I_c is the moment of inertia of PM; K_d is a damping factor; $\eta(t)$ is an unknown term such as external disturbances and remodeled dynamics of PM; r_1 and r_2 are two values for arm of force. In this paper, $r_1 = r_2 = R$.

According to (1), (2) and (3), $T(t)$ can be written as

$$\begin{aligned} T =& k_0 u_0 R(4k_{f1}\varepsilon_0 R l_0^{-1} + 2k_{f2} R l_0^{-1})\theta(t) + \\ & k_0 k_u R(2k_{f1}\varepsilon_0^2 + 2k_{f1} R^2 l^{-2}\theta^2(t) + \\ & 2k_{f2}\varepsilon_0 + 2k_{f3})V' + \eta(t), \end{aligned} \tag{4}$$

where $k_{f1}R^2 l_0^{-2}\theta^2(t)u(t)$ is considered in $\eta(t)$.

Then, according to (3) and (4), the dynamic model of PM mechanism can be written as

$$\begin{aligned} \ddot{\theta}(t) =& \frac{2k_0 k_v R(k_{f1}\varepsilon_0^2 + k_{f2}\varepsilon_0 + k_{f3})}{I_c} V' + d(\theta, t) - \\ & \frac{K_d}{I_c}\dot{\theta}(t) + \frac{2k_0 u_0 R^2(2k_{f1}\varepsilon_0 + k_{f2}) l_0^{-1}}{I_c}\theta(t). \end{aligned} \tag{5}$$

B. System transformation

Recalling (5), let $y_1(t) = \theta(t)$, $y_2(t) = \dot{\theta}(t)$. Then, the system of the PM joint can be obtained as

$$\begin{cases} \dot{y}_1 = y_2, \\ \dot{y}_2 = d_1 y_1(t) + d_2 y_2(t) + b_0 V' + d(\theta, t), \\ V' = D(u), \end{cases}$$

where, $b_0 = 2k_0 k_u R(k_{f1}\varepsilon_0^2 + k_{f2}\varepsilon_0 + k_{f3})I_c$, $d_1 = 2k_0 u_0 R^2(2k_{f1}\varepsilon_0 + k_{f2}) l_0^{-1} I_c$, $d_2 = K_d I_c^{-1}$.

Let $g(y_1, y_2) = d_1 y_1(t) + d_2 y_2(t)$. Then, the system can be written as

$$\begin{cases} \dot{y}_1 = y_2, \\ \dot{y}_2 = g(y_1, y_2) + b_0 V' + d(\theta, t), \\ V' = D(u). \end{cases}$$

C. Preliminaries

According to the universal approximation property of NNs, the unknown nonlinear function $M(X)$ can be written as $g(X) = V^{*T}\Psi(W^{*T}X) + \epsilon$, where V^* is an ideal weight matrix between hidden layer and output layer; W^* is an ideal weight matrix between the input layer and hidden layer; ϵ is the network reconstruction error. Considering threshold effect, the activation function is $\Psi(x) = [\overline{\Psi}(x), 1]^T \in R^m$, where $[\overline{\Psi}(x)]_i = \frac{1}{1+e^{x_i}}$, $i = 1, \cdots, m$, here m is the number of neurons in the hidden layer.

Without loss of generality, make the following assumption: W is the weight matrix between the input layer and the hidden layer of the actual feed-forward neural network (FNN), V is the weight matrix between the hidden layer and the output layer of the actual FNN, m is the number of neurons in the hidden layer. The output of three-layer FNN can be written as

$$g(X, W, V) = V^T \Psi(W^T X). \tag{6}$$

Considering threshold effect, the activation function is $\Psi(W^T X) = [\overline{\Psi}(W^T X), 1]^T \in R^{m+1}$, $[\overline{\Psi}(x)]_i = \frac{1}{1+e^{x_i}}, i = 1, \cdots, m$.

Lemma 1. *[30] For a three-layer FNN, if its two weight matrices are adjusted at the same time. The approximation error satisfies the following equality:* $g(X, W, V) - g(X) = \tilde{V}^T(\Psi - \Psi' W^T X) + V^T \Psi' \tilde{W}^T X + \Theta$, *where* $\tilde{W} = W - W^*$, $\tilde{V} = V - V^*$, Ψ *and* Ψ' *are short for* $\Psi(W^T X)$ *and* $\partial_{\Psi(x)}/\partial_x|_{x=W^T X}$. $\Theta = \tilde{V}^T \Psi' W^{*T} X - V^{*T} o_\Psi(\cdot) - \epsilon$, $o_\Psi(\cdot)$ *represents the higher order term of* $\Psi(W^{*T}X)$ *in Taylor expansion of* $W^T X$.

Lemma 2. *[30] If a three-layer FNN is set as* (6)*, and Lemma 1 holds, the following inequality holds* $|\Theta| \le \zeta^* P$, *where* ζ^* *is an unknown finite constant,* $P = 1 + \|X\| + \|W\|\|X\| + \|V\|\|X\|$.

Lemma 3. *[31] The following inequality is true, that is* $-2\beta tr\{\theta\tilde{\theta}^T\} \le -\beta|\tilde{\theta}|^2 + \beta|\theta^*|^2$, *where* $\tilde{\theta} = \theta - \theta^*$, *here* $\tilde{\theta}$ *and* θ *are vectors or matrices with the same dimension,* β *is an arbitrary constant.*

Lemma 4. *[24] If the following inequality is true, that is* $0 < \frac{\partial_D}{\partial_u} < 2$, *then there exists a unique* u_{dl}^* *satisfies* $h(u_{dc}, u_{dr}, u_{dl}^*) \triangleq \eta(u_{dc} - u_{dl}^* + u_{dr}) - u_{dl}^* = 0$.

III. Adaptive controller design

A. The basic form of adaptive controller

In this paper, the target trajectory is defined as $\theta_d(t)$. Let $y_d(t) = \begin{bmatrix} y_{d1}(t) & y_{d2}(t) \end{bmatrix}^T = \begin{bmatrix} \theta_d(t) & \dot{\theta}_d(t) \end{bmatrix}^T$. The system's state tracking error vector $\Delta(t)$ is $\Delta(t) = y(t) - y_d(t)$. And the filter tracking error $r(t)$ is

$$r(t) = \begin{bmatrix} k & 1 \end{bmatrix} \Delta(t), \tag{7}$$

where k is the appropriate parameter to select. It makes the tracking error Δ tends to 0 when r tends to 0. Therefore, the derivative of the filtering tracking error is

$$\dot{r} = g(y_1, y_2) + V' + d + Y_d, \tag{8}$$

where $Y_d = -\dot{y}_{d2}(t) + k(y_2 - y_{d2}(t))$ is a known function for target trajectories and tracking errors. Because the unknown nonsymmetric dead-zone of the actuator is continuous, it is assumed that $V' = D'(u) + \epsilon_r$, where $D'(u)$ is an approximation of the unknown nonsymmetric actuator dead-zone. ϵ_r is the reconstruction error satisfying $|\epsilon_r| \le \epsilon_{rm}$. It can be obtained that

$$V' = u + \eta(u) + \epsilon_r, \tag{9}$$

where $\eta(u) = D'(u) - u$ is an unknown function. It can be approximated by a neural network. And the input of actuator be determined as

$$u = u_{dc} - u_{dl} + u_{dr}, \tag{10}$$

where u_{dc} is a control input to stabilize linearized dynamics, u_{dl} is the dead-zone compensation term constructed by using NNs, u_{dr} is the robust term. Substitute (10) into (9), it can be gotten that

$$V' = u_{dc} + \eta(u) - u_{dl} + u_{dr} + \epsilon_r. \tag{11}$$

If u_{dl} can completely counteract the effect of $\eta(u)$, u_{dr} completely cancels the reconstruction error ϵ_r, disturbance $d = 0$, then $V = u_{dc}$.

According to (8) and (11), the filtering error can be written as follows:

$$\dot{r}(t) = g(y_1, y_2) + u_{dc} - u_{dl} + u_{dr} + \eta + \epsilon_r + d + Y_d. \tag{12}$$

Because the nonlinear function $g(y_1, y_2)$ is unknown, we first give the control input u_{dc} as

$$u_{dc} = -\hat{g} - Y_d - K_r r(t), \tag{13}$$

where $\hat{g}$ is the approximate output of NNs of nonlinear function $g(y_1, y_2)$, its specific form is given in the next subsection.

B. Estimation of nonlinear dynamic behavior

The unknown nonlinear function $g(y_1, y_2)$ of the controlled system is estimated by an NN named NN1. For the network NN1, we suppose that the weight matrix between the hidden layer and the input layer is given randomly and no longer adjusted, and the weight matrix between the hidden layer and the output layer is adjusted according to the correction law given later, then $g(y_1, y_2) = V_a^{*T}\Psi(W_a^T Y_1)+\epsilon_1$, where W_a is the weight matrix between the input layer and the hidden layer, V_a^* is the ideal weight matrix between input layer and hidden layer, ϵ_1 is the network reconstruction error satisfying $|\epsilon_1| \leq \epsilon_{1m}$. The activation function is $\Psi_1(x) = [\bar{\Psi}_1(x), 1]^T \in R^{n+1}$, $[\bar{\Psi}_1(x)]_i = \frac{1}{1+e^{-x_i}}$, $i = 1, \cdots, n$, here n is the number of hidden layer nodes.

The actual output of NN1 is $\hat{g} = V_a^T \Psi_a(W_a^T Y_1)$, where $Y_1 = [y_1, y_2, 1]^T \in R^3$.

The update law of V_a can be designed as

$$\dot{V}_a = \gamma_{V_a} r(t)\Psi_a(W_a^T Y_1) - \gamma_{V_a} I_{V_a} V_a, \tag{14}$$

where γ_{V_a}, I_{V_a} are positive learning rates given by designer.

Therefore, the estimation error of NN1 can be expressed as

$$\hat{g} - g(y_1, y_2) = \tilde{V}_a^T \Psi_1 - \epsilon_1, \tag{15}$$

where $\tilde{V}_a = V_a - V_a^*$ is the estimation error of NN weight.

C. Actuator dead-zone compensator

In (10), u_{dl} is used to counteract the effect of dead-zone. That is, using an NN to get u_{dl} to counteract $\eta(u)$. Based on Lemma 4, a static NN can be substituted for a recurrent neural network (RNN) to approximate u_{dl}^*, which enables the controller to avoid solving the fixed point problem at every moment [24]. Therefore, a static NN named NN2 is used to approximate $\eta(u)$. According to the NN function approximation theory, $\eta(u)$ can be expressed as follows: $\eta(u) = V_b^{*T}\Psi_b(W_b^{*T} Y_2) + \epsilon_2$.

The output of NN2 is

$$u_{dl} = V_b^T \Psi_b(W_b^T Y_2), \tag{16}$$

where $Y_2 = [u_{dc},\ r(t)/\alpha,\ \xi,\ (\|W_b\| + \|V_b\|), 1]^T \in R^5$, here $r(t)/\rho$, ξ and $\|W_b\| + \|V_b\|$ are determined by the expression of u_{dr}.

The update law of V_b can be designed as

$$\begin{aligned}\dot{V}_b =&\gamma_{V_b} r(t)(\Psi_b(W_b^T Y_2)- \\ &\Psi_b'(W_b^T Y_2)W_b^T Y_2) - \gamma_{V_b} I_{V_b} V_b,\end{aligned} \tag{17}$$

and the update law of W_b can be designed as

$$\dot{W}_b = \gamma_{W_b} r(t) Y_2 V_b^T \Psi_b' - \gamma_{W_b} I_{W_b} W_b, \tag{18}$$

where $\gamma_{V_b}, \gamma_{W_b}, I_{V_b}, I_{W_b}$ are positive learning rates given by designer.

According to Lemma 1, the NN approximation error can be expressed as

$$u_{dl} - \eta = \tilde{V}_b^T(\Psi_b - \Psi_b' W_b^T Y_2) + V_b^T \Psi_b' \tilde{W}_b^T Y_2 + \delta(t), \tag{19}$$

where $\delta(t) = \tilde{V}_b^T \Psi_b' W_b^{*T} Y_2 - V_b^{*T} o_{\Psi_b}(\cdot) - \epsilon_2(t), \tilde{W}_b = W_b - W_b^*, \tilde{V}_b = V_b - V_b^*$ is the estimation error of NN weights.

According to Lemma 2, there is

$$|\delta| \leq \xi^* p, \tag{20}$$

where $\xi^* \in R$ is an unknown constant, $p = 1 + \|Y_2\| + \|W_b\|\|Y_2\| + \|V_b\|\|Y_2\|$.

D. Stability analysis

According to (12), (13), (15), (16) and (19), the derivative of the filtering error is

$$\begin{aligned}\dot{r}(t) =& - K_r r(t) - \hat{g} + (\eta - u_{dl}) + u_{dr} + \epsilon_s + d(t) \\ =& - K_r r(t) - \tilde{V}_a^T \Psi_a + \epsilon_1 - [V_b^T(\Psi_b - \\ &\Psi_b' W_b^T Y_2) + V_b^T \Psi_b' \tilde{W}_b^T Y_2 + \delta(t)] + \\ &u_{dr} + \epsilon_s + d(t),\end{aligned} \tag{21}$$

where the robust term is designed as

$$u_{dr} = -\zeta p \tanh(r(t)p/\alpha). \tag{22}$$

The update law of robust term is

$$\dot{\zeta} = \gamma_\zeta r(t) p \tanh(r(t)p/\alpha) - \gamma_\zeta I_\zeta \zeta, \tag{23}$$

where γ_ζ, I_ζ are positive learning rates given by designer.

Remark 1. *u_{dr} is used to overcome the unknown external disturbance. Different from [4], which needs to know the upper bound of the external disturbance in advance, the method in this paper does not need to know in advance, nor does it need offline estimation.*

Theorem 1. *For the internal pressure* (1)*, if the controller u_{dc} is designed as* (13)*, the dead-zone compensator u_{dl} is designed as* (16)*, the robust term of the system and its update law are designed as* (22) *and* (23)*, and the update laws of NNs are designed as* (14)*,* (17) *and* (18)*, the following fact is true: The tracking error and the weight estimation errors of NNs eventually converge to a compact set related to parameters. They can be adjusted to be small enough.*

Proof: Consider the following Lyapunov function:

$$\begin{aligned}\Gamma =&\frac{1}{2}r^2(t) + \frac{1}{2\gamma_{V_a}}\|\tilde{V}_a\|^2 + \frac{1}{2\gamma_{W_b}}\|\tilde{W}_b\|^2 + \\ &\frac{1}{2\gamma_{V_b}}\|\tilde{V}_b\|^2 + \frac{1}{2\gamma_\zeta}\|\zeta\|^2.\end{aligned} \tag{24}$$

The derivative of (24) is

$$\begin{aligned}\dot{\Gamma} =&r(t)\dot{r}(t) + \frac{1}{\gamma_{V_a}}\tilde{V}_a^T \dot{\tilde{V}}_a + \frac{1}{\gamma_{W_b}} tr\{\tilde{W}_b^T \dot{\tilde{W}}_b\} + \\ &\frac{1}{\gamma_{V_b}}\tilde{V}_b^T \dot{\tilde{V}}_b + \frac{1}{\gamma_\zeta}\zeta\dot{\zeta}.\end{aligned} \tag{25}$$

Recalling (20) and (21), we have

$$\begin{aligned}\dot{\Gamma} =& r(t)\Big\{-K_r r(t) - \tilde{V}_a^T\Psi_a + \epsilon_1 - \Big[V_b^T\Psi_b'\tilde{W}_b^T Y_2 + \\ & \tilde{V}_b^T(\Psi_b - \Psi_b' W_b^T Y_2) + \delta(t)\Big] + u_{dr} + \epsilon_s + d\Big\} + \\ & \frac{1}{\gamma_{V_a}}\tilde{V}_a^T\dot{\tilde{V}}_a + \frac{1}{\gamma_{W_b}}tr\{\tilde{W}_b^T\dot{\tilde{W}}_b\} + \frac{1}{\gamma_\zeta}\tilde{\zeta}\dot{\tilde{\zeta}} \\ \leq & - K_r r^2(t) + \tilde{V}_a^T(\frac{1}{\gamma_{V_a}}\dot{V}_a - r(t)\Psi_a) + \\ & tr\{\tilde{W}_b^T(\frac{1}{\gamma_{W_b}^T}\dot{W}_b - r(t)Y_2 V_b^T\Psi_b')\} + \\ & \tilde{V}_b^T(\frac{1}{\gamma_{V_b}}\dot{V}_b - r(t)(\Psi_b - \Psi_b' W_b^T Y_2)) + r(t)u_{dr} + \\ & |r(t)|(\zeta_0^* p + \epsilon_{sm} + d_m + \epsilon_{1m}) + \frac{1}{\gamma_\zeta}\tilde{\zeta}\dot{\tilde{\zeta}}. \end{aligned} \tag{26}$$

Substitute (22) and (23) into the above inequality, and let $\zeta^* = \xi^* + \epsilon_{sm} + \epsilon_{1m} + d_m$, it can be gotten that

$$\begin{aligned}\dot{\Gamma} \leq & - K_r r^2(t) + \tilde{V}_a^T\frac{1}{\gamma_{V_a}}\dot{V}_a - r\Psi_a + \\ & tr\{\tilde{W}_b^T(\frac{1}{\gamma_{W_b}}\dot{W}_b - r(t)Y_2 V_b^T\Psi_b')\} + \\ & \tilde{V}_b^T\frac{1}{\gamma_{V_b}}\dot{V}_b - r(t)(\Psi_b - \Psi_b' W_b^T Y_2) - \\ & \zeta r(t)p\tanh(r(t)p/\alpha) + |r(t)|\zeta^* p + \\ & \tilde{\zeta}r(t)p\tanh(r(t)p/\alpha) - K_\zeta\tilde{\zeta}\zeta. \end{aligned} \tag{27}$$

Substitute (14), (17) and (18) into it, we have

$$\begin{aligned}\dot{\Gamma} \leq & - K_r r^2(t) - \lambda_{V_a} tr\{\tilde{W}_a^T W_a\} - \\ & \lambda_{W_b} tr\{\tilde{W_b^T} W_b\} - \lambda_{V_b} tr\{\tilde{V}_b^T V_b\} - \\ & \xi r(t)p\tanh(r(t)p/\alpha) + |r(t)|\xi p - \lambda_\zeta\tilde{\zeta}\zeta. \end{aligned} \tag{28}$$

According to Lemma 3 and the inequality in [31], that is $0 \leq |x| - xtanh(x/\beta) \leq 0.2785\beta$, where $\beta > 0$, $x \in R$, we have

$$\begin{aligned}\dot{\Gamma} \leq & - K_r r^2(t) + 0.2785\rho\xi - \frac{I_{V_a}}{2}\|\tilde{V}_a\|^2 + \\ & \frac{I_{V_a}}{2}\|V_a^*\|^2 - \frac{I_{W_b}}{2}\|\tilde{W}_b\|^2 + \frac{I_{W_b}}{2}\|W_b^*\|^2 - \\ & \frac{I_{V_b}}{2}\|\tilde{V}_b\|^2 + \frac{I_{V_b}}{2}\|V_b^*\|^2 - \frac{I_\zeta}{2}|\tilde{\zeta}|^2 + \frac{I_\zeta}{2}|\zeta^*|^2 \\ \leq & - K_r r^2(t) - \frac{I_{V_a}}{2}\|\tilde{V}_a\|^2 - \frac{I_{W_b}}{2}\|\tilde{W}^b\|^2 - \\ & \frac{I_{V_b}}{2}\|\tilde{V}_b\|^2 - \frac{I_\zeta}{2}|\tilde{\zeta}|^2 + B, \end{aligned} \tag{29}$$

where $B = \frac{I_{V_a}}{2}\|V_a^*\|^2 + \frac{I_{W_b}}{2}\|W_b^*\|^2 + \frac{I_{V_b}}{2}\|V_b^*\|^2 + \frac{I_\zeta}{2}|\zeta^*|^2 + 0.2785\rho\xi^*$.

Let $A = \min\{2K_r, I_{V_a}\gamma_{V_a}, I_{W_b}\gamma_{W_b}, I_{V_b}\gamma_{V_b}, I_\zeta\gamma_\zeta\}$, we have $\dot{\Gamma} \leq -A\Gamma + B$. Multiply both sides by e^{At}, it can be obtained that $\frac{d}{dt}(\Gamma(t)e^{At}) \leq e^{At}B$. According to [32], integrating the above inequality over $[0, t]$, we have

$$\Gamma(t) \leq (\Gamma(0) - \frac{B}{A})e^{-At} + \frac{B}{A} \leq \Gamma(0) + \frac{B}{A}. \tag{30}$$

Therefore, combined with (24), it can be obtained that $|r| \leq \sqrt{2\Gamma(0) + 2B/A}$, $\|\tilde{V}_a\| \leq \sqrt{2\gamma_{V_a}(\Gamma(0) + B/A)}$, $\|\tilde{W}_b\| \leq \sqrt{2\gamma_{W_b}(\Gamma(0) + B/A)}$, $\|\tilde{V}_b\| \leq \sqrt{2\gamma_{V_b}(\Gamma(0) + B/A)}$, $|\tilde{\zeta}| \leq \sqrt{2\gamma_\zeta(\Gamma(0) + B/A)}$.

Let $\upsilon = 2\Gamma(0) + 2B/A$. From (7), we have $r(t) = k\Delta_1(t) + \Delta_2(t)$. And there is a normal number c satisfying $|\Delta^{-kt}| \leq c\Delta^{-kt}$. Because $\Delta = [\Delta_1 \ \Delta_2]^T$, it can be obtained that $\|\Delta\| \leq |\Delta_1| + |\Delta_2| \leq (1+k)|\Delta_1| + |r|$, $\|\Delta\| \leq c(1 + |k|)|\Delta_1(0)| + \left[1 + \frac{(1+k)c}{k}\right]\sqrt{\upsilon}$. Because $\Delta_1(0) = 0$, it can be obtained $\|\Delta\| \leq \left[1 + \frac{(1+k)c}{k}\right]\sqrt{\upsilon}$.

Let $\bar{\upsilon} = [1 + \frac{(1+k)c}{k}]\sqrt{\upsilon}$. Therefore, the consistent boundedness of the system state and NN weight parameters can be obtained as follows: $\|y(t)\| \leq \|\Delta(t)\|$, $\|V_a\| \leq \sqrt{\gamma_{V_a}\upsilon} + \|V_a^*\|$, $\|W_b\| \leq \sqrt{\gamma_{W_b}\upsilon} + \|W_b^*\|$, $\|V_b\| \leq \sqrt{\gamma_{V_b}\upsilon} + \|V_b^*\|$, $|\zeta| \leq \sqrt{\gamma_\zeta\upsilon} + |\zeta^*|$.

Furthermore, from (30), we have $\Gamma(t) \leq \left[\Gamma(0) - \frac{B}{A}\right]e^{-At} + \frac{B}{A}$. Let $\upsilon' = 2B/A$, we have $\lim_{t\to\infty}\Gamma(t) = \frac{1}{2}\upsilon'$.

Similarly, the consistent final boundedness of the tracking error of the closed-loop system and the weight parameters of NNs can be deduced as follows: $\lim_{t\to\infty}\|\Delta(t)\| = \bar{\upsilon}'$, $\lim_{t\to\infty}\|\tilde{V}_a\| = \sqrt{\gamma_{V_a}\upsilon'}$, $\lim_{t\to\infty}|\tilde{\zeta}| = \sqrt{\gamma_\zeta\upsilon'}$, $\lim_{t\to\infty}\|\tilde{W}_b\| = \sqrt{\gamma_{W_b}\upsilon'}$, $\lim_{t\to\infty}\|\tilde{V}_b\| = \sqrt{\gamma_{V_b}\upsilon'}$, where $\bar{\upsilon}' = \left[1 + \frac{(1+k)c}{k}\right]\sqrt{\upsilon'}$. ■

Remark 2. *This paper uses an NN to estimate the system state online for real-time tracking. This is different from the reference auxiliary signal processing error in [4], which improves the tracking speed of the system and reduces the system state error.*

IV. Simulation studies

In order to prove the feasibility of the controller in this paper, a numerical analysis is carried out on a same PM system as in [4], which is shown in Fig. 1. The initial parameters of the PM system are $b_{10} = 2$, $d_{11} = 0.1$, $d_{12} = 0.65$, $b_{20} = 3$, $d_{21} = 0.88$, and $d_{22} = 0.3$.

The structure of neural network NN1 is 3-11-1. The structure of neural network NN2 is 5-21-1. The initial values of the weight V_a of NN1 and the weight V_b of NN2 are placed at -0.1. And the initial values of the weight W_a of NN1 and the weight W_b of NN2 are set to 0.1. Estimated parameter ξ is 0.01.

The initial parameters of the controller are $k = 8$, $K_v = 10$, $I_{V_a} = 0.005$, $I_{V_b} = -0.005$, $I_{W_b} = -0.005$, $I_\zeta = 0.05$, $\gamma_{V_a} = 0.9$, $\gamma_{V_b} = 0.9$, $\gamma_{W_b} = 0.3$, $\gamma_\zeta = 0.1$, and $\alpha = 0.01$.

The initial condition is set to $y = [1\ 0]^T$. And $d(y,t) = 0.2\sin(y_1 + y_2)\cos(t)$. In this paper, choose the target trajectory $\theta_d(t) = \sin(t)$. The following two cases are considered.

A. Case 1

Let $b_0 = b_{10}$, $d_1 = d_{11}$, $d_2 = d_{12}$. When $b_1 = b_2 = 0$, the controller is a general actuator without dead-zone. The simulation results are shown in Fig. 2 and 3. The tracking performance and the tracking error are shown in the Fig. 2. It can be observed that the deviation between the power angle and the ideal operating point is almost 0 during the transient process. And it also can be seen that the tracking error drops rapidly and smoothly to around 0. Fig. 3 shows the output of the actuator.

By comparing Fig. 2 and Fig. 1 in [4], it can be concluded that there are better tracking performance and transient

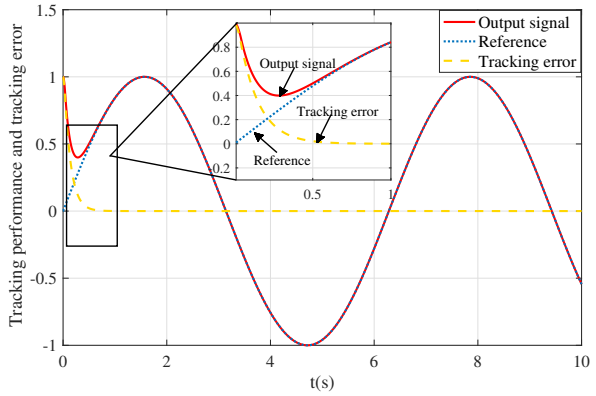

Fig. 2: The tracking performance and the tracking error without actuator dead-zone in Case 1.

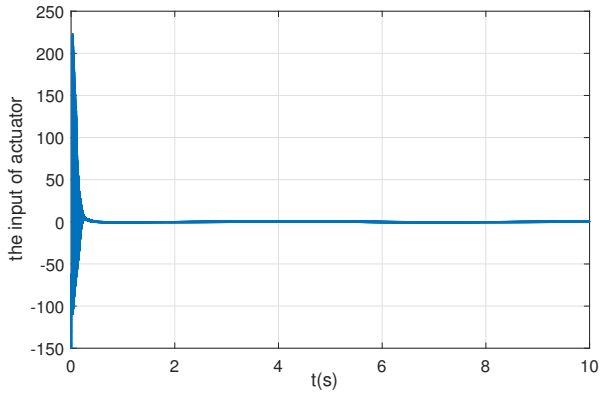

Fig. 3: The output of actuator without dead-zone in Case 1.

performance than [4]. From Fig. 3, it is discernible that the actuator output adheres to the system's constraint requirements Moreover, this approach takes into account the actuator dead-zone issue, which was not addressed in [4].

According to Fig. 3, the dead-zone nonlinearity of the actuator can be set as follows: $b_1 = -3$, $b_2 = 4$, $m_1(u) = u - b1$, $m_2(u) = u - b_2$. The simulation results are shown in Fig. 4, 5 and 6. The tracking performance and error with actuator dead-zone of the system are shown in Fig. 4. State y_2 with actuator dead-zone is shown in Fig. 5. The input and output of actuator with actuator dead-zone are shown in Fig. 6.

Based on the figures obtained in Case 1, the following conclusions can be drawn.

1) After a comparison of Fig. 4 and Figure 1 in [4], it can be seen that the actuator with dead-zone designed in this paper can get better results than those obtained in [4].
2) By comparing Fig. 4 and 2, and Fig. 6 and 3 respectively, it can be seen that the results with actuator dead-zone are almost no different from the results without actuator dead-zone in this paper.

B. Case 2

Let $b_0 = b_{20}$, $d_1 = d_{21}$, $d_2 = d_{22}$. The simulation results (including tracking performance, tracking error, state y_2 and the input and the output of actuator) are shown in Fig. 7, 8 and 9. Based on the simulation figures, the results obtained by the control method in this paper are independent of the unknown system parameters b_0, d_1, d_2. When the system parameters change, the method proposed in this paper can still ensure the stable tracking of the system.

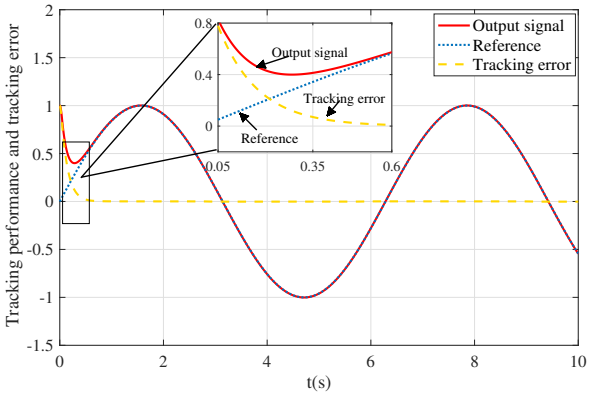

Fig. 4: The tracking performance and the tracking error with actuator dead-zone in Case 1.

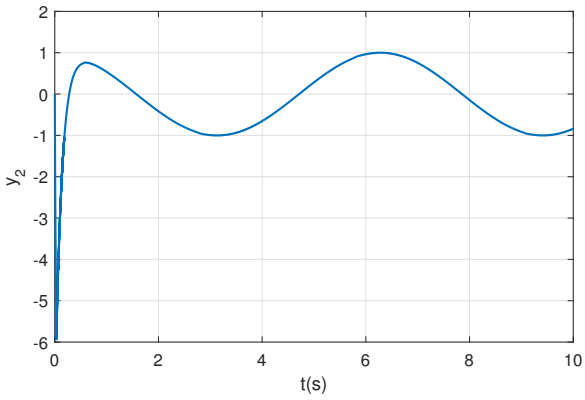

Fig. 5: State y_2 with actuator dead-zone in Case 1.

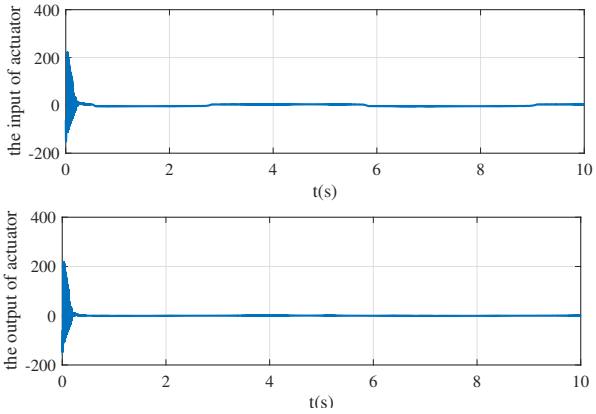

Fig. 6: The input and the output of actuator in Case 1.

V. Conclusion

This paper employs a design framework for an adaptive neural network (NN) finite-time controller to effectively address the inherent challenges of pneumatic muscles. This framework leverages real-time estimation of system states and external disturbances to enable online estimation of system errors, significantly enhancing the tracking performance

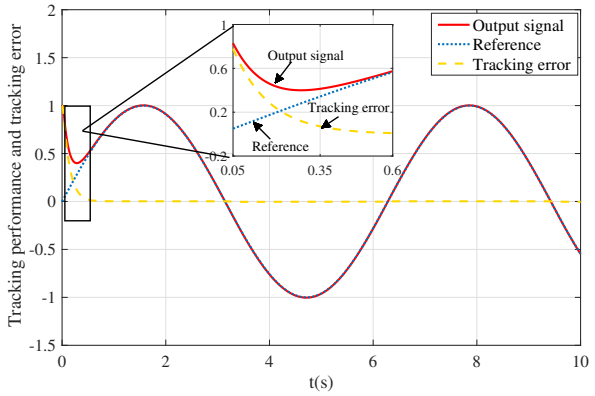

Fig. 7: The tracking performance and the tracking error with actuator dead-zone in Case 2.

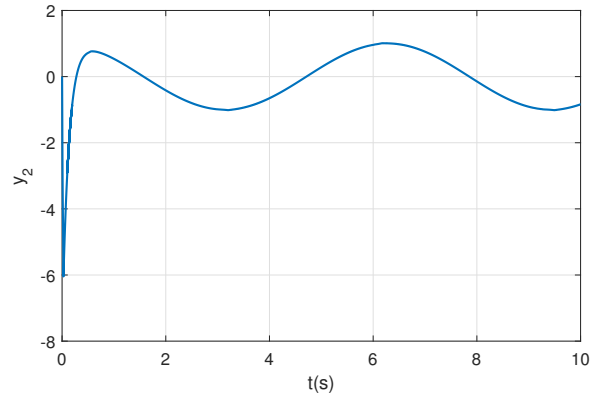

Fig. 8: State y_2 with actuator dead-zone in Case 2.

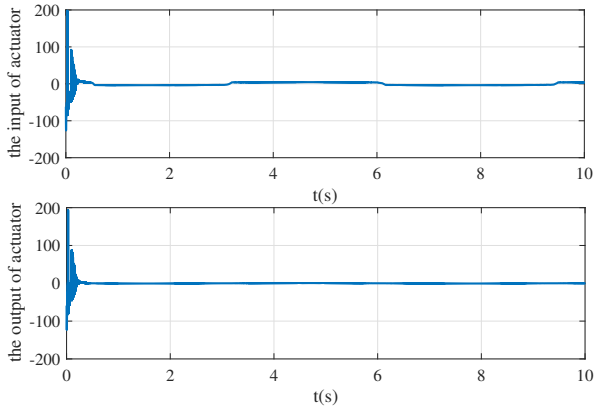

Fig. 9: The input and the output of actuator with actuator dead-zone in Case 2.

of pneumatic muscles. To tackle the dead-zone issue within the nonlinear characteristics of actuators, a static neural network compensator is introduced, effectively mitigating these challenges. The research findings indicate that the tracking error of the closed-loop system and the weight parameters of the NN exhibit ultimate uniform boundedness, and the system's tracking error will converge to a small neighborhood with an adjustable radius. Simulation results further validate the feasibility and effectiveness of the controller in meeting the system's requirement for actuator output boundedness.

REFERENCES

[1] Y. Wen, J. Si, A. Brandt, X. Gao, and H. Huang, "Online reinforcement learning control for the personalization of a robotic knee prosthesis," *IEEE Transactions on Cybernetics*, vol. 50, no. 6, pp. 2346–2356, 2020.

[2] L. Zhao, H. Cheng, Y. Xia, and B. Liu, "Angle tracking adaptive backstepping control for a mechanism of pneumatic muscle actuators via an aeso," *IEEE Transactions on Industrial Electronics*, vol. 66, no. 6, pp. 4566–4576, 2019.

[3] S. Hussain, P. K. Jamwal, M. H. Ghayesh, and S. Q. Xie, "Assist-as-needed control of an intrinsically compliant robotic gait training orthosis," *IEEE Transactions on Industrial Electronics*, vol. 64, no. 2, pp. 1675–1685, 2017.

[4] J.-P. Cai, F. Qian, R. Yu, and L. Shen, "Adaptive control for a pneumatic muscle joint system with saturation input," *IEEE Access*, vol. 8, pp. 117 698–117 705, 2020.

[5] Z. Zhu, Y. Pan, Q. Zhou, and C. Lu, "Event-triggered adaptive fuzzy control for stochastic nonlinear systems with unmeasured states and unknown backlash-like hysteresis," *IEEE Transactions on Fuzzy Systems*, vol. 29, no. 5, pp. 1273–1283, 2021.

[6] H. Liang, X. Guo, Y. Pan, and T. Huang, "Event-triggered fuzzy bipartite tracking control for network systems based on distributed reduced-order observers," *IEEE Transactions on Fuzzy Systems*, vol. 29, no. 6, pp. 1601–1614, 2021.

[7] J. Cai, R. Yu, Q. Yan, C. Mei, B. Wang, and L. Shen, "Event-triggered adaptive control for tank gun control systems," *IEEE Access*, vol. 7, pp. 17 517–17 523, 2019.

[8] Z. Yao, J. Yao, and W. Sun, "Adaptive rise control of hydraulic systems with multilayer neural-networks," *IEEE Transactions on Industrial Electronics*, vol. 66, no. 11, pp. 8638–8647, 2019.

[9] B. Fan, Q. Yang, S. Jagannathan, and Y. Sun, "Output-constrained control of nonaffine multiagent systems with partially unknown control directions," *IEEE Transactions on Automatic Control*, vol. 64, no. 9, pp. 3936–3942, 2019.

[10] W. He, C. Xue, X. Yu, Z. Li, and C. Yang, "Admittance-based controller design for physical human-robot interaction in the constrained task space," *IEEE Transactions on Automation Science and Engineering*, vol. 17, no. 4, pp. 1937–1949, 2020.

[11] W. He, T. Wang, X. He, L.-J. Yang, and O. Kaynak, "Dynamical modeling and boundary vibration control of a rigid-flexible wing system," *IEEE/ASME Transactions on Mechatronics*, vol. 25, no. 6, pp. 2711–2721, 2020.

[12] Q. Liang, Q. Yang, W. Meng, and Y. Li, "Adaptive finite-time control for turbo-generator of power systems with prescribed performance," *Asian Journal of Control*, vol. 24, no. 4, pp. 1597–1608, 2021.

[13] T. Ma, "Decentralized filtering adaptive neural network control for uncertain switched interconnected nonlinear systems," *IEEE Transactions on Neural Networks and Learning Systems*, vol. 32, no. 11, pp. 5156–5166, 2021.

[14] F. Beltran-Carbajal, R. Tapia-Olvera, A. Valderrabano-Gonzalez, and I. Lopez-Garcia, "Adaptive neuronal induction motor control with an 84-pulse voltage source converter," *Asian Journal of Control*, vol. 23, no. 4, pp. 1603–1616, 2020.

[15] D. Liu, X. Ouyang, N. Zhao, and Y. Luo, "Adaptive event-triggered control with prescribed performance for nonlinear system with full-state constraints," *IAENG International Journal of Applied Mathematics*, vol. 54, no. 3, pp. 390–397, 2024.

[16] R. Hamed, A. Mohammad, and E. Mohsen, "Continuous nonsingular terminal sliding mode control based on adaptive sliding mode disturbance observer for uncertain nonlinear systems," *Automatica*, vol. 109, p. 108515, 2019.

[17] Q. Su, W. Quan, G. Cai, and J. Li, "Improved adaptive backstepping sliding mode control for generator steam valves of non-linear power systems," *IET Control Theory & Applications*, vol. 11, no. 9, pp. 1414–1419, 2017.

[18] T. Zhou, S. Zhai, C. Li, and H. Peng, "Fully distributed leaderless consensus of general nonlinear multi-agent systems with directed topology and bounded disturbances," *IAENG International Journal of Applied Mathematics*, vol. 54, no. 1,

pp. 40–46, 2024.

[19] M. Zhang, P. Shi, C. Shen, and Z.-G. Wu, "Static output feedback control of switched nonlinear systems with actuator faults," *IEEE Transactions on Fuzzy Systems*, vol. 28, no. 8, pp. 1600–1609, 2020.

[20] N. Sun, Y. Fu, T. Yang, J. Zhang, Y. Fang, and X. Xin, "Nonlinear motion control of complicated dual rotary crane systems without velocity feedback: Design, analysis, and hardware experiments," *IEEE Transactions on Automation Science and Engineering*, vol. 17, no. 2, pp. 1017–1029, 2020.

[21] Z. Gong, D. Huang, H. U. K. Jadoon, L. Ma, and W. Song, "Sensor-fault-estimation-based tolerant control for single-phase two-level pwm rectifier in electric traction system," *IEEE Transactions on Power Electronics*, vol. 35, no. 11, pp. 12 274–12 284, 2020.

[22] D. Huang, Y. Fu, N. Qin, and S. Gao, "Fault diagnosis of high-speed train bogie based on lstm neural network," *Science China Information Sciences*, vol. 64, no. 1, 2020.

[23] Y. Wu, B. Jiang, and Y. Wang, "Incipient winding fault detection and diagnosis for squirrel-cage induction motors equipped on crh trains," *ISA Transactions*, vol. 99, pp. 488–495, 2020.

[24] Y. Luo, H. Zhang, and Q. Zhang, "Neural network adaptive controller design for a class of affine nonlinear system with unknown nonsymmetric actuator dead-zone," *ACTA ELECTRONICA SINICA*, vol. 36, no. 11, p. 7, 2008.

[25] H. Wang, B. Chen, C. Lin, and Y. Sun, "Observer-based adaptive fuzzy tracking control for a class of mimo nonlinear systems with unknown dead zones and time-varying delays," *International Journal of Systems Science*, vol. 50, no. 3, pp. 546–562, 2019.

[26] Y. Li, H. Cheng, J. Wang, and Y. Wang, "Dynamic analysis of unilateral diffusion gompertz model with impulsive control strategy," *Advances in Difference Equations*, vol. 2018, no. 1, 2018.

[27] K. He, C. Dong, and Q. Wang, "Active disturbance rejection adaptive control for uncertain nonlinear systems with unknown time-varying dead-zone input," *Asian Journal of Control*, vol. 24, no. 3, pp. 1209–1222, 2022.

[28] Z. Liu, G. Lai, Y. Zhang, and C. L. P. Chen, "Adaptive fuzzy tracking control of nonlinear time-delay systems with dead-zone output mechanism based on a novel smooth model," *IEEE Transactions on Fuzzy Systems*, vol. 23, no. 6, pp. 1998–2011, 2015.

[29] J. Wang, H. Cheng, H. Liu, and Y. Wang, "Periodic solution and control optimization of a prey-predator model with two types of harvesting," *Advances in Difference Equations*, vol. 2018, no. 1, 2018.

[30] J.-H. Park, S.-H. Huh, S.-H. Kim, S.-J. Seo, and G.-T. Park, "Direct adaptive controller for nonaffine nonlinear systems using self-structuring neural networks," *IEEE Transactions on Neural Networks*, vol. 16, no. 2, pp. 414–22, 2005.

[31] T. Zhang and S. S. Ge, "Adaptive neural control of mimo nonlinear state time-varying delay systems with unknown dead-zones and gain signs," *Automatica*, vol. 43, no. 6, pp. 1021–1033, 2007.

[32] S. S. Ge and C. Wang, "Adaptive neural control of uncertain mimo nonlinear systems," *IEEE Transactions on Neural Networks*, vol. 15, no. 3, pp. 674–92, 2004.